

**IN PLANE VIBRATIONS OF CURVED  
TIMOSHENKO BEAMS WITH VARIABLE  
CURVATURE**

**A Thesis Submitted to  
the Graduate School of Engineering and Sciences of  
İzmir Institute of Technology  
in Partial Fulfillment of the Requirements for the Degree of**

**MASTER OF SCIENCE**

**in Mechanical Engineering**

**by  
Uğur CİN**

**March 2016  
İZMİR**

We approve the thesis of **Uğur CİN**

**Examining Committee Members:**

---

**Prof. Dr. Bülent YARDIMOĞLU**

Department of Mechanical Engineering, İzmir Institute of Technology

---

**Assist. Prof. Dr. Onursal ÖNEN**

Department of Mechanical Engineering, İzmir Institute of Technology

---

**Assoc. Prof. Dr. Levent MALGACA**

Department of Mechanical Engineering, Dokuz Eylül University

**29 March 2016**

---

**Prof. Dr. Bülent YARDIMOĞLU**

Supervisor, Department of Mechanical Engineering,  
İzmir Institute of Technology

---

**Prof. Dr. Metin TANOĞLU**

Head of the Department of  
Mechanical Engineering

---

**Prof. Dr. Bilge KARAÇALI**

Dean of the Graduate School  
of Engineering and Sciences

## **ACKNOWLEDGEMENTS**

First of all, I would like to express my deep gratitude to my thesis advisor; Prof. Dr. Bulent YARDIMOGLU for his patience, motivation, enthusiasm, immense knowledge and sustained support during my MSc thesis study. He was a great pathfinder in all the time of research and writing processes of this thesis; so it's unimaginable to have a better advisor and mentor than him for the studies.

## **ABSTRACT**

### **IN PLANE VIBRATIONS OF CURVED TIMOSHENKO BEAMS WITH VARIABLE CURVATURE**

In this study, in-plane vibrations of curved Timoshenko beams with variable curvature is studied by Finite Element Method. In the selected method, it is known that generalized differential eigenvalue problem are solved by reducing the equations from continuous to discrete domain. Catenary form is used as the axis of curved beam. An APDL (ANSYS Parametric Design Language) code is developed for the geometric and finite element models of the curved beam. The computer code is validated by the data available in the literature. After validation of developed computer code, the effects of parameters, which are related to shape of the curved beam, on the natural frequencies and mode shapes are studied.

## ÖZET

### DEĞİŞKEN EĞRİLİKLİ EĞRİ TIMOŞENKO ÇUBUKLARIN DÜZLEM İÇİ TITREŞİMLERİ

Bu çalışmada, değişken eğrilikli eğri Timoshenko çubukların düzlem içi titreşimleri Sonlu Elemanlar Yöntemi ile incelenmiştir. Seçilen yöntem de , eğri çubuğun genelleştirilmiş diferansiyel özdeğer problemi, denklemlerin sürekli ortamdan ayrık ortama indirgenmesi ile çözülmüştür. Eğri çubuğun ekseni olarak Katenary biçimi kullanılmıştır. Eğri çubuğun geometrik ve sonlu eleman modeli APDL (ANSYS Parametrik Tasarım Dili) kodu ile geliştirilmiştir. Bilgisayar kodu literatürde mevcut veiller ile doğrulanmıştır. Bilgisayar kodunun doğrulanmasından sonra, eğri çubuğun şekli ile ilişkili parametrelerin doğal frekans ve doğal titreşim biçimlerine etkileri çalışılmıştır.

# TABLE OF CONTENTS

LIST OF FIGURES .....	vii
LIST OF TABLES.....	viii
LIST OF SYMBOLS .....	ix
CHAPTER 1. GENERAL INTRODUCTION .....	1
CHAPTER 2. THEORETICAL VIBRATION ANALYSIS.....	7
2.1. Introduction.....	7
2.2. Mathematical Model of Catenary .....	8
2.3. Equation of Motion of Timoshenko Curved Beam .....	9
2.4. Modal Analysis by Finite Element Method.....	12
2.5. Description of Beam188 Finite Element .....	12
CHAPTER 3. RESULTS AND DISCUSSIONS .....	16
3.1. Introduction.....	16
3.2. Convergence Studies for Model .....	17
3.3. Verification of APDL Code.....	18
3.4. Modal Analysis for Different Models.....	19
CHAPTER 4. CONCLUSIONS .....	26
REFERENCES .....	27

## LIST OF FIGURES

<b><u>Figure</u></b>	<b><u>Page</u></b>
Figure 1.1. Simply supported beam .....	1
Figure 1.2. Beam bending differential element .....	2
Figure 1.3. Two and three dimensional curves .....	3
Figure 1.4. Curved beam with uniform and tapered cross-section .....	3
Figure 1.5. A curved beam having variable radius of curvature.....	3
Figure 1.6. Archimedes-type spiral spring.....	5
Figure 1.7. Arch geometry and loads on an arch element .....	6
Figure 2.1. Non circular curved beam .....	7
Figure 2.2. Different catenary forms by hanging chains .....	7
Figure 2.3. Parameters of catenary curve .....	8
Figure 2.4. Curved beam coordinates and stress resultants for in plane vibration .....	10
Figure 2.5. Nodes of BEAM188 .....	13
Figure 2.6. Cross Section Subtypes .....	14
Figure 2.7. Coordinate system of BEAM188 .....	14
Figure 2.8. BEAM188 Element Gauss integration points .....	15
Figure 3.1. The geometrical model of the curved beam with $R_0=80$ mm.....	16
Figure 3.2. Convergence of first natural frequency .....	18
Figure 3.3. Opening angle $\theta_0$ of circular curved beam .....	19
Figure 3.4. Effects of $b$ and $R_0$ on first natural frequencies.....	19
Figure 3.5. Effects of $b$ and $R_0$ on second natural frequencies .....	20
Figure 3.6. Effects of $b$ and $R_0$ on third natural frequencies.....	20
Figure 3.7. Effects of $b$ and $R_0$ on fourth natural frequencies .....	21
Figure 3.8. Effects of $R_0$ and $b$ on first natural frequencies.....	21
Figure 3.9. Effects of $R_0$ and $b$ on second natural frequencies .....	22
Figure 3.10. Effects of $R_0$ and $b$ on third natural frequencies.....	22
Figure 3.11. Effects of $R_0$ and $b$ on fourth natural frequencies .....	23
Figure 3.12. First natural mode shape.....	23
Figure 3.13. Second natural mode shape .....	24
Figure 3.14. Third natural mode shape .....	24
Figure 3.15. Fourth natural mode shape .....	24
Figure 3.16. Fifth natural mode shape .....	25

## LIST OF TABLES

<b><u>Table</u></b>	<b><u>Page</u></b>
Table 3.1. Material properties.....	17
Table 3.2. Convergence of first natural frequencies.....	17
Table 3.3. Comparison of first natural frequency parameters $\lambda$ .....	18



## LIST OF SYMBOLS

$A$	cross-sectional area
$E$	modulus of elasticity
$f_i$	$i^{\text{th}}$ natural frequency
$G$	shear modulus
$I$	second moment of area
$[K]$	stiffness matrix
$L [ \ ]$	differential operator for stiffness
$M$	bending moment
$M [ \ ]$	differential operator for mass
$[M]$	mass matrix
$N$	number of element
$Q$	shear force
$s$	circumferential coordinate
$s_L$	length of the beam
$(x_r, z_r)$	the tip co-ordinates of the curved beam
$y$	displacement of straight beam
$\alpha, \alpha_r$	slope of the curve at any point and point r
$\varepsilon$	tangential strain due to tension
$\kappa$	shear correction factor
$\emptyset$	rotation due to bending moment
$\gamma$	shear angle
$\mu$	density of mass
$\rho_0(z), \rho_0(\alpha), \rho_0(s)$	variable radius of curvature
$\omega$	natural frequency
$( \ ` )$	derivative with respect to “s”
$( \ . )$	derivative with respect to “t”

# CHAPTER 1

## GENERAL INTRODUCTION

Beam is very crucial structural member due to the common usage in practice. Since the objects have elastic behavior in their daily usage, it bends under the lateral loads. Bending forms are related with the boundary conditions of the beam. Figure 1.1 shows a simply supported beam as unloaded and loaded at midpoint by force  $F$ .

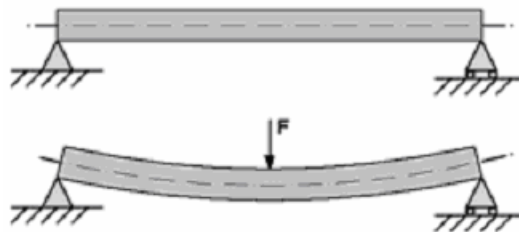


Figure 1.1. Simply supported beam

In 18th century, the first beam theory regarding transverse motion was developed. Jacob Bernoulli found curvature-bending moment relationship. His nephew Daniel Bernoulli extended this study for vibrations of beams. Later, Leonhard Euler studied on displacements of beams under typical loading. Therefore, this first beam theory is called as Euler-Bernoulli beam theory. Due to the simplicity and accuracy provided by its assumptions, this theory gives reasonable solutions for practical engineering problems. This beam theory is also called as classical beam theory.

The second beam theory appeared in 1877. This theory is known as the Rayleigh beam theory and based on the inclusion of the effect of rotation of the cross-section, namely rotary inertia.

Euler-Bernoulli beam theory is extended to Shear beam theory by considering the shear force effects in bending.

Timoshenko proposed a new beam theory by combining the all effect mentioned above. Therefore, in this beam theory, classical beam theory is modified by including the shear deformation and rotary inertia of the beam. The original figure from the paper of

Timoshenko is given in Figure 1.2. In this figure,  $\phi$  and  $\gamma$  represent the rotation of the cross-section due to the bending moment and shear force, respectively.

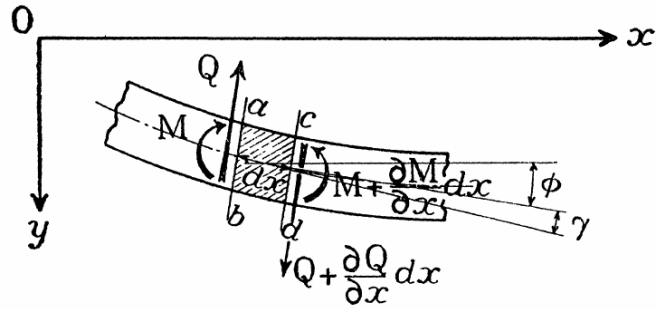


Figure 1.2. Beam bending differential element  
(Source: Timoshenko 1921)

Rotatory inertia term given below is added to differential equation.

$$\text{Rotatory inertia term} = I \mu (\partial^2 y / \partial x^2 \partial t^2) \quad (1.1)$$

where,  $I$  is second moment of area of the cross section,  $\rho$  is the mass density,  $y$  is deflection curve, and  $t$  is time. Another contribution of this theory is related with the definition of deflection which is given by (Timoshenko 1921)

$$\frac{\partial y}{\partial x} = \phi + \gamma \quad (1.2)$$

Moreover, bending moment and shear force are given as follows:

$$M = -EI \frac{\partial \phi}{\partial x} \quad (1.3)$$

and

$$Q = \kappa AG \gamma \quad (1.4)$$

or

$$Q = \kappa AG \left( \frac{\partial y}{\partial x} - \phi \right) \quad (1.5)$$

The aspect ratio of beam is an important parameter for the usage of proper beam theory. For thin beams, Euler-Bernoulli beam theory gives acceptable accurate results. However, for stubby/thick beam, Timoshenko beam theory provides more accurate results.

Curved beams are used in lot of applications depending on their shape. They may be two or three dimensional curve as shown in Figure 1.3. Moreover, they may have tapering cross-section or/and variable curvature. Their geometry is formed by considering the functional and esthetical aims. Figure 1.4 and Figure 1.5 show curved beam with uniform and tapered cross-section and curved beam having variable radius of curvature, respectively.

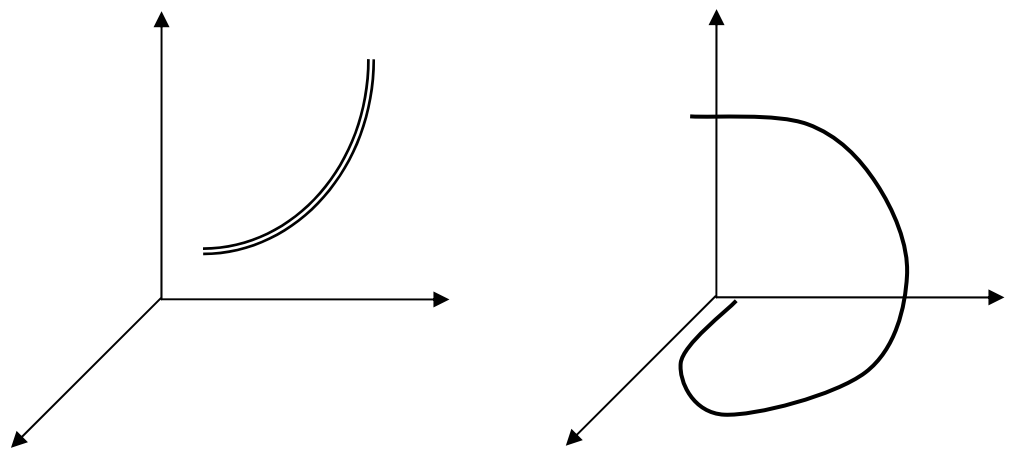


Figure 1.3. Two and three dimensional curves

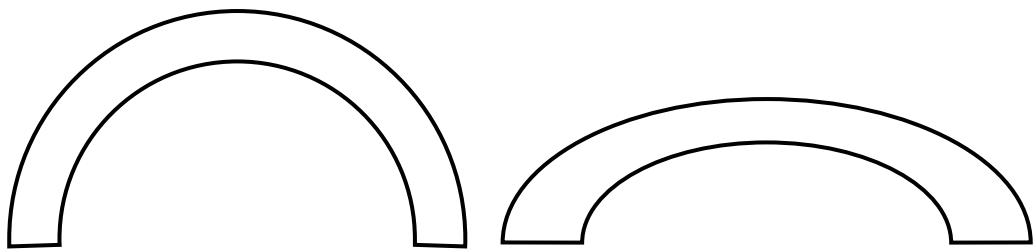


Figure 1.4. Curved beam with uniform and tapered cross-section

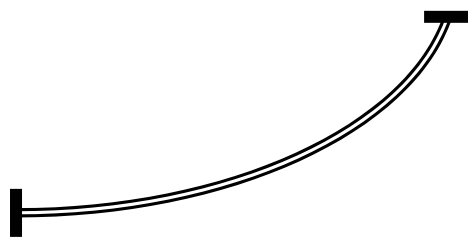


Figure 1.5. A curved beam having variable radius of curvature

Curved beams may have in-plane or out-of plane vibrations: In the first one, it has in-plane bending, extensional or axial displacements. Bending and axial motions are naturally related, then their differential equations are coupled. For simplification these coupled equation can be uncoupled. To uncouple the differential equations, in extensionality condition is assumed. According to this assumption, axial strain in neutral axis is zero. To discuss this assumption, lots of researches were carried out as experimentally and theoretically. So, it is possible to find these discussions in the literature.

If the curved beam has out-of-plane vibration, it has out-of-plane bending and torsional displacements. Again, similar to first case, aforementioned displacements are coupled. However, they are not uncoupled.

There are different curved beam theories based on straight beam theories. The oldest and simplest one is based on Bernoulli-Euler beam theory. Relatively new one is based on Timoshenko beam Theory. According to this beam theory, as discussed before, shear deformation and rotary inertia are considered in the differential equations of the motion. While Euler beam can be modeled by only one differential equation, Timoshenko beam model have two coupled differential equations.

It is possible to find numerous studies on vibrations of circular curved beams modeled by Bernoulli-Euler and Timoshenko beam theories. However, curved beams having variable curvature modeled by Timoshenko beam theory are limited. The selected reachable ones are summarized in the order of publication time as follows:

Den Hartog (1928) derived an expression for the first and second natural frequencies of a part of a circular ring, hinged or clamped at both ends. He shown that the type of vibration, in which extension of the fibers occurs, under certain conditions may have a lower natural frequency than the non-extensional type of vibration.

Den Hartog's study (1928) was extended by Volterra and Morell (1960). They used Rayleigh-Ritz method to analyze the free vibration of arches with various geometries such as circle, cycloid, catenary, and parabola.

Tseng et al (1997) provided a systematic approach to solve in-plane free vibrations of arches with variable curvature by introducing the concept of dynamic stiffness matrix into a series solution for in-plane vibrations of arches with variable curvature. An arch is divided into as many elements as needed for accuracy of solution. In each element, a series solution is formulated in terms of polynomials, the coefficients of which are related to each other through recurrence formulas. In the whole analysis, the effects of rotary inertia and shear deformation have been taken into account.

Yıldırım (1997) found the natural frequencies of Archimedes-type spirals illustrated in Figure 1.6 by using the transfer matrix method. In her study, the shear deformation and rotary inertia are taken into account. She used the complementary functions method to compute the overall dynamic transfer matrix and concluded that the solution method can be applied to any planar bar.

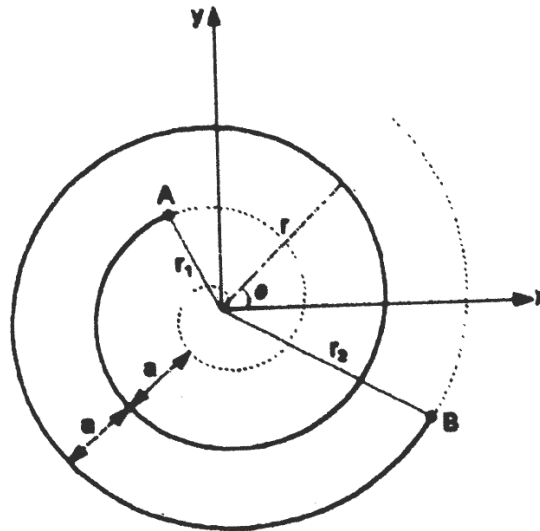


Figure 1.6. Archimedes-type spiral spring  
(Source: Yıldırım 1997)

Irie et al (1983) calculated frequency parameters of clamped-clamped arcs having different opening angles by using Transfer matrix method. They considered two different cross-sectioned Timoshenko curved beams: rectangular cross-sectioned and circular cross-sectioned.

Kang et al (1995) found the in-plane and out-of plane vibration frequencies of circular arches based on the Bresse-Timoshenko beam theory by using the differential quadrature method. They verified their results by the results of Irie et al (1983).

Huang et al (1998) studied on in plane vibration of arches with variable curvature as well as cross section, considering the shear deformation and rotary inertia effects. They developed an exact solution by using Frobenius method combined with dynamic stiffness method, and then provided some non-dimensional frequencies of parabolic arches based on the rise to span length, slenderness ratio, and variation of cross section.

Oh et al. (1999) obtained the governing differential equations for free in-plane vibrations of non-circular arches including the rotatory inertia, shear deformation and axial deformation effects. Figure 1.7 shows the arch geometry in their study. Figure 1.7 also

shows a small element of the arch with internal forces and moments under the external effect. They used numerical methods to find the natural frequencies. The lowest four natural frequencies are calculated for the non-circular shape such as parabolic, elliptic and sinusoidal geometries with hinged-hinged, hinged-clamped, and clamped-clamped end conditions. A wide range of arch rise to span length ratios, slenderness ratios, and two different values of shear parameter are also considered. Their numerical results are in good agreement with results determined by means of finite element method.

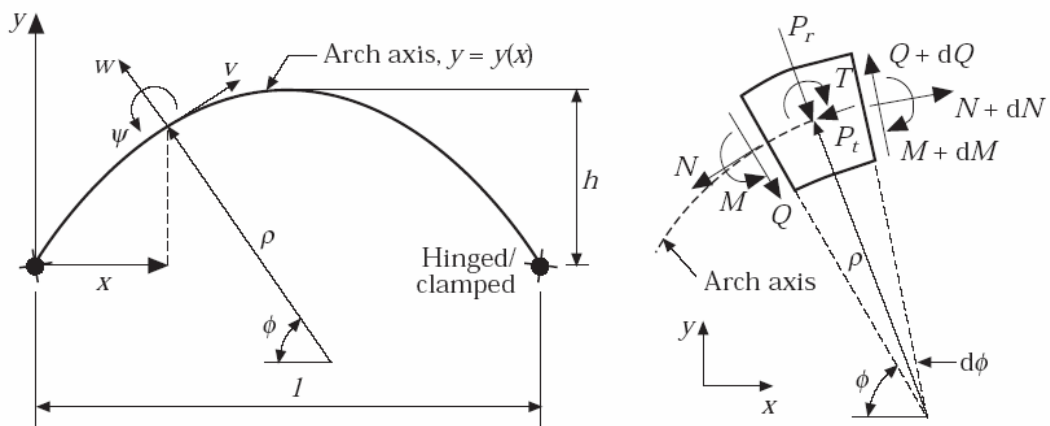


Figure 1.7. Arch geometry and loads on an arch element  
(Source: Oh *et al.* 1999)

In this study, in-plane vibrations of curved Timoshenko beams with variable curvature is analyzed by numerical methods since the differential equation coefficients are not constant. Generalized differential eigenvalue problem of curved beam are solved by reducing the equations from continuous to discrete domain. Catenary form is used as the axis of curved beam. An APDL (ANSYS Parametric Design Language) code is developed for the geometric and finite element models of the curved beam in the study. The computer code is validated by the data available in the literature. After validation of developed computer code, the effects of curvature parameters on the natural frequencies and mode shapes are studies.

## CHAPTER 2

### THEORETICAL VIBRATION ANALYSIS

#### 2.1. Introduction

A non circular curved beam is illustrated in Figure 2.1. In practice, catenary form shown in Figure 2.2 is very common. It describes a wire, rope, or chain hanging freely from two points. If the curvature is not constant, the equations of motion of the Timoshenko curved beam have variable coefficients. Thus, their solution can be obtained in numerical methods due to the difficulty in analytical methods. Finite Element Method's the most common one.

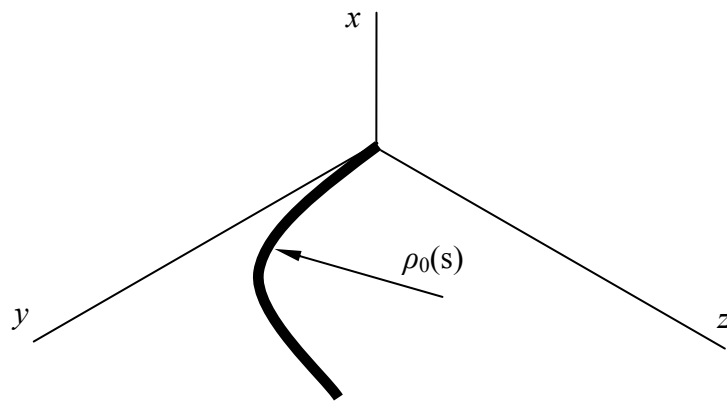


Figure 2.1. Non circular curved beam



Figure 2.2. Different catenary forms by hanging chains



## 2.2. Mathematical Model of Catenary

The mathematical model of catenary can be found generally in the textbook on statics as the equilibrium shape of free-hanging chains. A catenary curve with parameters shown in Figure 2.3 given by Yardimoglu (2010) is considered.

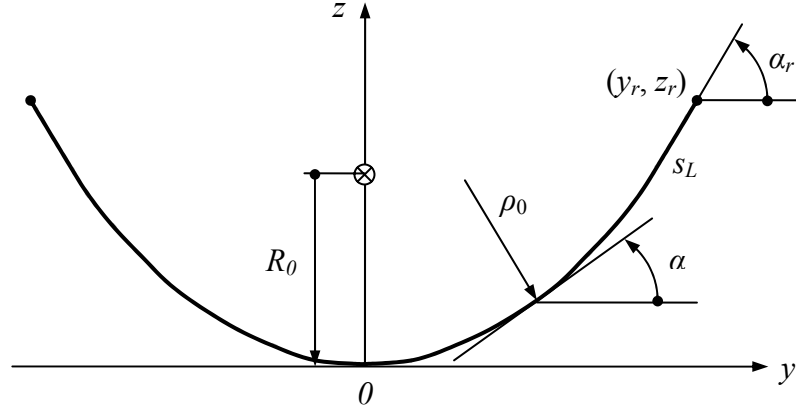


Figure 2.3. Parameters of catenary curve  
(Source: Yardimoglu 2010)

The mathematical function of a catenary curve in  $y$ - $z$  plane is expressed as

$$z(y) = R_0[\cosh(y/R_0) - 1] \quad (2.1)$$

The slope  $\alpha$  is obtained as:

$$\tan \alpha = dz(y)/dy = \sinh(y/R_0) \quad (2.2)$$

It is possible to find  $y_r$  by using the tip slope  $\alpha_r$  as

$$y_r = R_0 \operatorname{arc} \sinh(\tan \alpha_r) \quad (2.3)$$

$$z_r = R_0 (1/\cos \alpha_r - 1) \quad (2.4)$$

On the other hand, the arc length  $s$  from origin 0 to any point  $(y, z)$  on the curve is

$$s(y) = \int_0^s \sqrt{1 + (dz(y)/dy)^2} dy = R_0 \tan \alpha \quad (2.5)$$

Thus, Equation 2.5 gives a very useful relationship between  $s$  and  $\alpha$ . From differential calculus, radius of curvature is given as

$$\rho_0(y) = \frac{[1 + (dz(y)/dy)^2]^{3/2}}{d^2z(y)/dy^2} = R_0 \cosh^2(y/R_0) \quad (2.6)$$

The variable  $y$  in Equation 2.6 can be eliminated by using Equation 2.2, then

$$\rho_0(\alpha) = R_0 / \cos^2 \alpha \quad (2.7)$$

It should be noted that  $\cos \alpha$  can be expressed in terms of  $s$  by using Equation 2.5

$$\cos \alpha = R_0 / \sqrt{R_0^2 + s^2} \quad (2.8)$$

Finally, radius of curvature is expressed in terms of  $s$  as

$$\rho_0(s) = R_0 + s^2 / R_0 \quad (2.9)$$

### 2.3. Equation of Motion of Timoshenko Curved Beam

There are two main beam theories. The majority of the studies are based on the thin beam theory expressed by Euler-Bernoulli beam theory which states that plane cross-sections remains plane during deformation. Another theory is thick beam theory developed by Timoshenko (1921). In this thick beam theory, shear deformation and rotary inertia are taken into consideration. For thick curved beam, it is accepted that the ratio of the radius of curvature to the in-plane thickness is greater than about 10. (Chidamparam and Leissa, 1993)

Curved beam with co-ordinate system, displacements, internal forces and moments shown in Figure 2.4 is considered. The positive senses for all the quantities are as indicated in the same figure. The radius of curvature  $\rho$  is assumed to be a function of  $s$ , i.e.,  $\rho = \rho(s)$ . As in Timoshenko beam theory, the total rotation of the centroidal axis (denoted by  $\omega$ ) is assumed to be composed of a part due to bending (denoted by  $\psi$ ) and a part due to

transverse shear effects. Using the Newton's second law, three differential equations are found as (Chidamparam and Leissa, 1993)

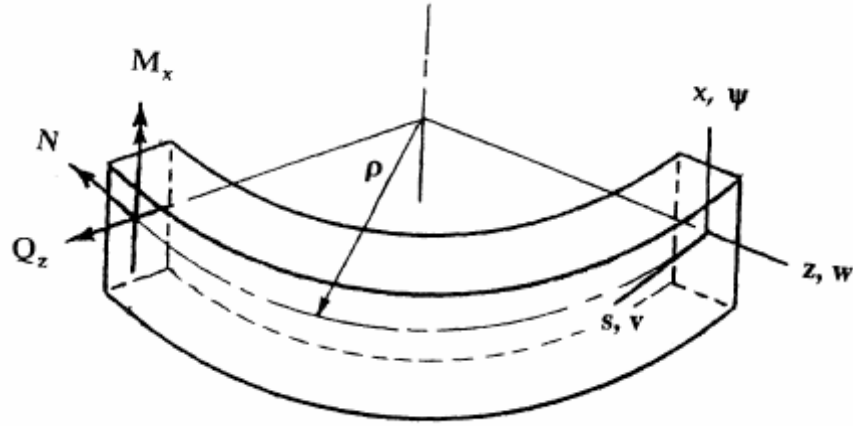


Figure 2.4. Curved beam coordinates and stress resultants for in plane vibration.  
(Source: Chidamparam and Leissa, 1993)

$$N' + \frac{Q_z}{\rho(s)} = \mu A \ddot{v} \quad (2.10)$$

$$Q_z' - \frac{N}{\rho(s)} = \mu A \ddot{w} \quad (2.11)$$

$$M_x' + Q_z = \mu I_x \ddot{\psi} \quad (2.12)$$

where primes and dots denote derivatives with respect to the arc length  $s$  and time, respectively.  $\mu$  represents density of mass. For small motions, the extensional strain  $\varepsilon$  and the rotation  $\omega$  of the centroidal axis are given by:

$$\varepsilon = v' + \frac{w}{\rho(s)} \quad (2.13)$$

$$\omega = w' - \frac{v}{\rho(s)} \quad (2.14)$$

$$N = EA\varepsilon = EA\left(v' + \frac{w}{\rho(s)}\right) \quad (2.15)$$

$$M_x = EI_x \psi' \quad (2.16)$$

where  $I_x$  is the second moment of area of the cross section of the curved beam. The shear force-shear strain relation is due to Timoshenko beam theory is written as

$$Q_z = \kappa AG(\omega - \psi) = \kappa AG\left(w' - \frac{v}{\rho(s)} - \psi\right) \quad (2.17)$$

where  $\kappa$  is the shear coefficient of the cross-section.

Substituting Equations (2.15)–(2.17) into Equations (2.10)–(2.12) and assuming a uniform cross-section and constant material properties through the curved beam yields

$$EA v'' - \frac{\kappa GA}{\rho(s)^2} v - \frac{\kappa GA}{\rho(s)} \psi + \frac{A(E + \kappa G)}{\rho(s)} w' + EA w \left[ \frac{1}{\rho(s)} \right]' = \mu A \ddot{v} \quad (2.18)$$

$$\kappa GA w'' - \frac{EA}{\rho(s)^2} w - \kappa GA \psi' - \frac{A(E + \kappa G)}{\rho(s)} v' - \kappa GA v \left[ \frac{1}{\rho(s)} \right]' = \mu A \ddot{w} \quad (2.19)$$

$$EI \psi'' - \kappa GA \psi - \frac{\kappa GA v}{\rho(s)} + \kappa GA w' = \mu I_x \ddot{\psi} \quad (2.20)$$

Equations (2.18) to (2.20) are the governing equations for in-plane free vibrations of beams with variable curvature given by also Tseng et al (1997).

The boundary conditions are of a curved beam can be written physically as:

$$\text{Either } M_x=0 \text{ (pinned or free), or } \psi=0 \text{ (clamped)} \quad (2.21)$$

$$\text{Either } Q_z=0 \text{ (free), or } w=0 \text{ (pinned or clamped)} \quad (2.22)$$

$$\text{Either } M_x=0 \text{ (pinned or free), or } w=0 \text{ (pinned or clamped)} \quad (2.23)$$

## 2.4. Modal Analysis by Finite Element Method

The governing equation of motion of a continuous system is given in general form having operators notation by Yardimoglu (2012)

$$M [\ddot{v}(s,t)] + L[v(s,t)] = 0 \quad (2.24)$$

where  $L[ ]$  and  $M[ ]$  are linear differential operators of derivatives with respect to  $s$ . Equation of motion in continuous domain given by Equation 2.241 is reduced to discrete domain by Finite Element Method that is detailed in excellent textbook written by Petyt (2010). Therefore, equation of motion of the curved beam is expressed as

$$[M] \{\ddot{x}(t)\} + ([K] + [G]) \{x(t)\} = 0 \quad (2.25)$$

where  $[M]$ ,  $[K]$  and  $[G]$  are mass matrix, elastic stiffness matrix and geometric stiffness matrix, respectively.  $\{x(t)\}$  is displacement vector. It is well-known that Equation 2.24 gives the eigenvalue problem which is expressed as

$$([K] + [G] - \omega_i^2 [M]) \{u_i\} = \{0\} \quad (2.26)$$

where  $\omega_i$  is  $i^{th}$  natural frequency and  $\{u_i\}$  is the  $i^{th}$  vibration mode shape vector.

## 2.5. Description of Beam188 Finite Element

BEAM188 can be used for analyzing both slender and moderately stubby/thick beams. Therefore, it is based on general case for beam theory which is Timoshenko beam theory. Linearly tapered beam may be modeled by this finite element.

BEAM188 has two nodes, I and J, in 3-D as shown in Figure 2.5. Nodal freedoms at each node are translations  $u$ ,  $v$ , and  $w$  in the  $x$ ,  $y$ , and  $z$  directions and rotations  $\theta_x$ ,  $\theta_y$ , and  $\theta_z$  about the  $x$ ,  $y$ , and  $z$  directions, respectively. The shape functions of this element are linear due to the two nodes and given as follows (Kohnke 2004):

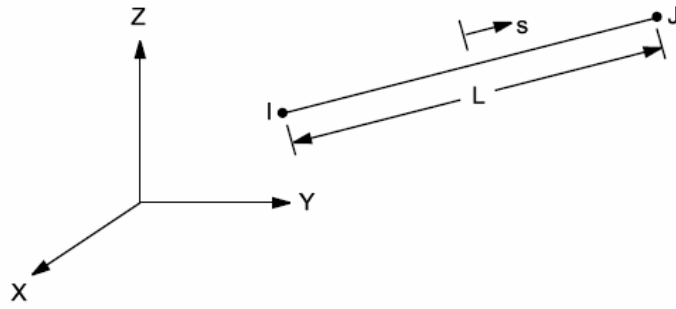


Figure 2.5. Nodes of BEAM188  
(Source: Kohnke 2004)

$$u = \frac{1}{2}[u_I(1-s) + u_J(1+s)] \quad (2.27)$$

$$v = \frac{1}{2}[v_I(1-s) + v_J(1+s)] \quad (2.28)$$

$$w = \frac{1}{2}[w_I(1-s) + w_J(1+s)] \quad (2.29)$$

$$\theta_x = \frac{1}{2}[\theta_{xI}(1-s) + \theta_{xJ}(1+s)] \quad (2.30)$$

$$\theta_y = \frac{1}{2}[\theta_{yI}(1-s) + \theta_{yJ}(1+s)] \quad (2.31)$$

$$\theta_z = \frac{1}{2}[\theta_{zI}(1-s) + \theta_{zJ}(1+s)] \quad (2.32)$$

In Equations from (2.27) to (2.32),  $s$  shows the distance from the midpoints of the element. For more details about this element, the papers of Simo and Vu-Quoc (1986) and Ibrahimbegovic (1995) are referred by Kohnke (2004).

Depending on the KEYOPT, warping can also be considered. Moreover, linear analysis and studies on large rotations or large nonlinear strain can be accomplished by this element. Additionally, flexural, lateral, and torsional stability problems can be analyzed.

Cross-sections for this element can be defined via SECTYPE, SECDATA, SECOFFSET, SECWRITE, and SECREAD. Common sections, such as rectangular, circular, I, L, T, Z, etc are available. All possible cross-sections are shown in Figure 2.6.

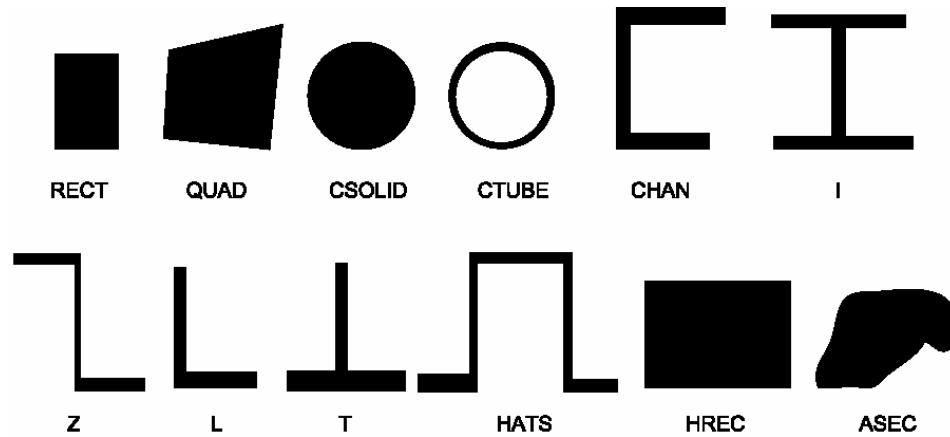


Figure 2.6. Cross Section Subtypes  
(Source: Ansys 2005)

User defined transverse shear stiffness can be entered via SECCONTROLS command. Otherwise, default shear coefficient is unity.

The coordinate system, geometry, and locations of nodes I, J, and K to define the element in the global coordinate system are shown in Figure 2.7. The orientation of the element is provided by node K.

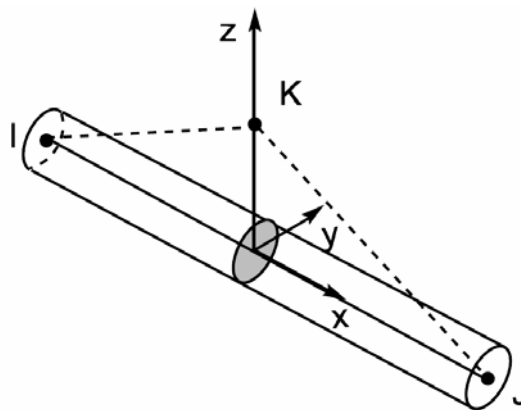


Figure 2.7. Coordinate system of BEAM188  
(Source: Kohnke 2004)

Gauss integration points along the length of the beam are shown in Figure 2.8. The strains, forces and bending moments associated with section are found at Gauss integration points.

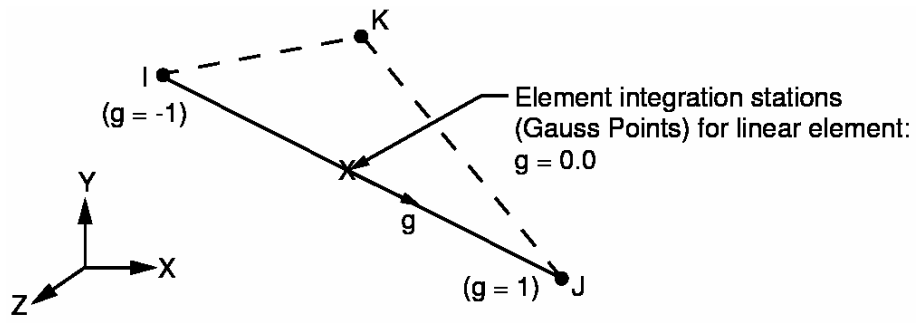


Figure 2.8. BEAM188 Element Gauss integration points  
(Source: Ansys 2007)



## CHAPTER 3

### NUMERICAL RESULTS AND DISCUSSION

#### 3.1. Introduction

In this chapter, in-plane vibration of a curved beam with variable curvature is analyzed by FEM (Finite Element Method).

APDL (ANSYS Parametric Design Language) is used to develop a code for a geometrical and finite element model. BEAM188 is used to model the curved Timoshenko beam.

Timoshenko curved beams having the parameters  $R_o = \{80, 100, 120\}$  mm,  $s_L = 200$  mm  $b = \{20, 24, 28, 32\}$  mm,  $h = 20$  mm are modeled. The cross-section dimension perpendicular curved beam plane is represented by  $h$ . One of the curved beam model in ANSYS is shown in Figure 3.1.

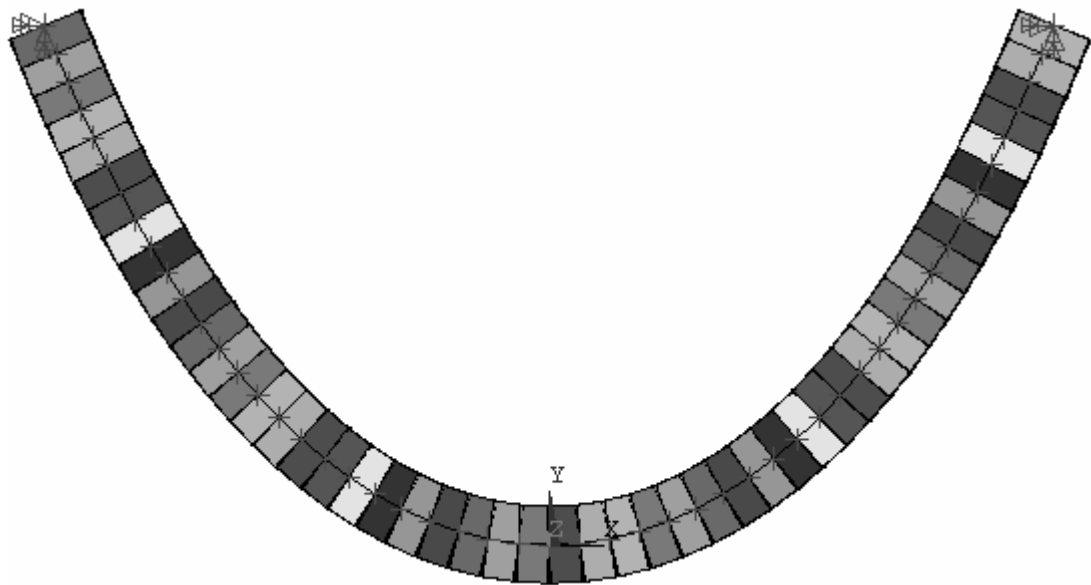


Figure 3.1. The geometrical model of the curved beam with  $R_o = 80$  mm

### 3.2. Convergence Studies for Model

To determine the minimum number of element in FEM, Timoshenko curved beam having the geometrical parameters  $b=20$  mm,  $h =20$  mm,  $R_o=80$  mm,  $s_L=200$  mm is modeled. The material properties of the curved beam used throughout the thesis are given in Table 3.1.

Table 3.1. Material properties

$E$ (MPa)	208000
$\rho$ (ton/mm <sup>3</sup> )	$7.85 \cdot 10^{-9}$
$G$ (MPa)	80000
$\nu$ (-)	0.3
$\kappa$ (-)	0.85

Modal analyses are performed in ANSYS by using different number of elements. The first natural frequencies are tabulated in Table 3.2. It is seen from Table 3.2 that the minimum number of element  $N$  can be selected as 50. Convergence curve of first natural frequency is plotted in Figure 3.2 which convergences to selected value.

Table 3.2. Convergence of first natural frequencies

$N$	$f_1$ (Hz)
20	1303.6
24	1296.3
30	1290.4
40	1285.8
50	1283.5
60	1282.6

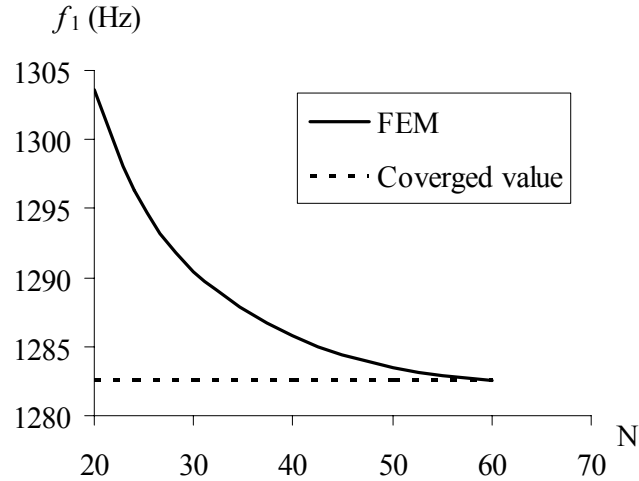


Figure 3.2. Convergence of first natural frequency

### 3.3. Verification of APDL Code

APDL code based on BEAM188 is tested by the natural frequencies of the Timoshenko circular curved beam with rectangular cross-section since there are no available results regarding the catenary curved beam model used in this study. As presented in Section 2.2, intrinsic equation of catenary is used to model it. Therefore, for this purpose, the results of Irie et al (1983) and Kang et al (1993) are used. The present results and the results of Irie et al (1983) and Kang et al (1993) in terms of their frequency parameter  $\lambda = \sqrt{\mu A \rho^4 \omega^2 / EI_x}$  and slenderness ratios  $s_x = \sqrt{A \rho^2 / I_x}$  are given in Table 3.3 for comparisons. In Table 3.3, is opening angle  $\theta_0$  of the circular curved beam and shown in Figure 3.3.

Table 3.3. Comparison of first natural frequency parameters  $\lambda$

$s_x$	$\theta_0$ (°)	Present	Irie et al (1983)	Kang et al (1995)
100	60	53.85	52.78	52.80
100	120	11.84	11.79	11.79
100	180	4.38	4.37	4.38

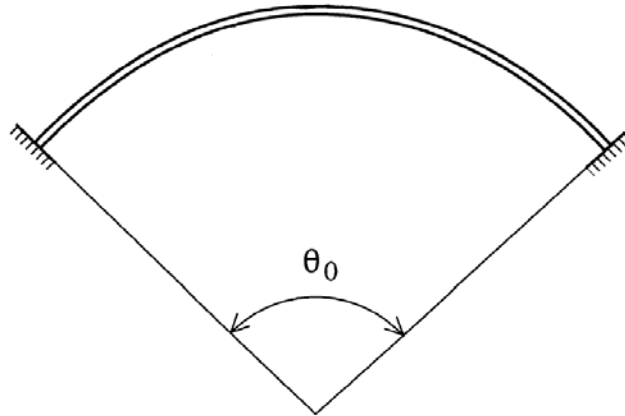


Figure 3.3. Opening angle  $\theta_0$  of circular curved beam

### 3.4. Modal Analysis for Different Models

The effects of catenary curve parameter  $R_o$  and the height of the cross-section  $h$  of the curved beam on natural frequencies can be seen in a selected range for those parameters. The other parameters are  $h=20$  mm,  $s_L=200$  mm are taken. The first, second, third, and fourth natural frequencies are given in Figures 3.4, 3.5, 3.6, and, 3.7, respectively.

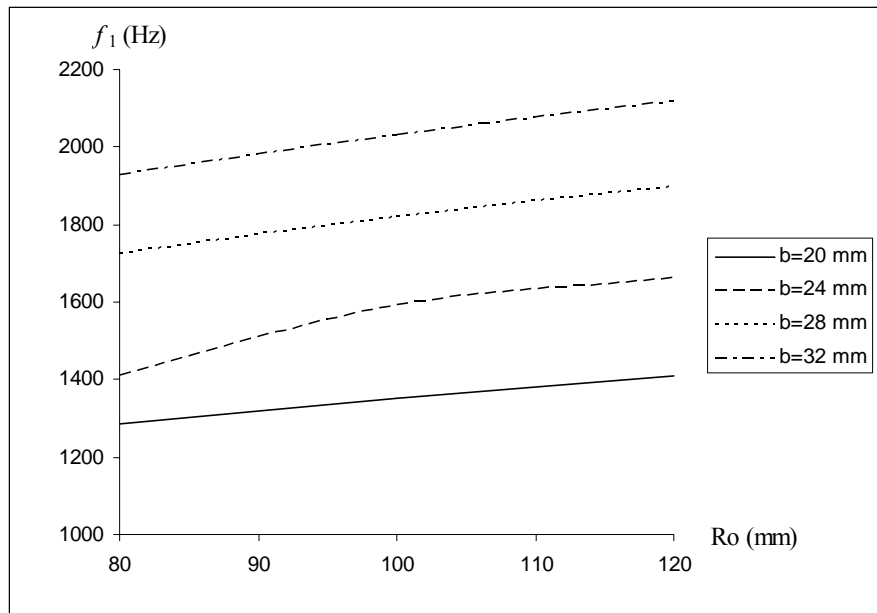


Figure 3.4. Effects of  $b$  and  $R_o$  on first natural frequencies

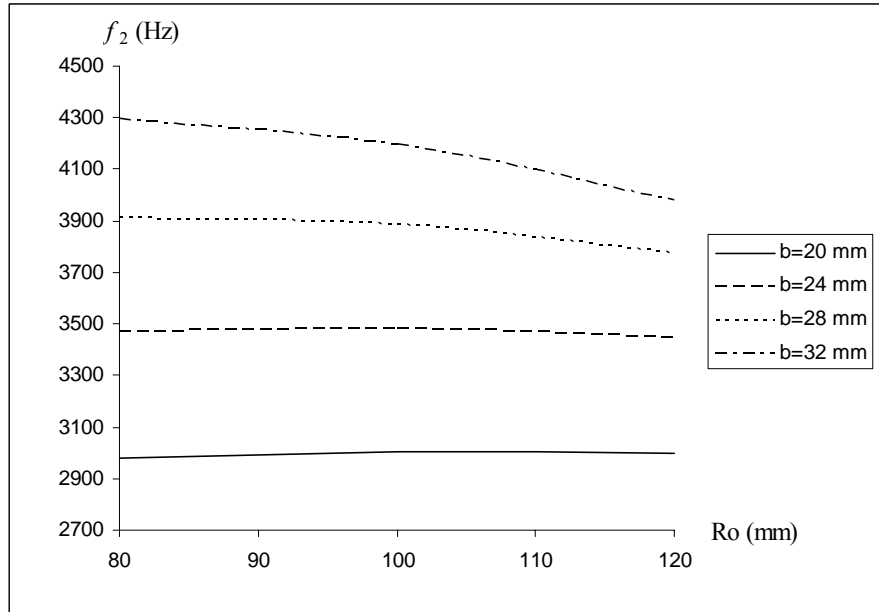


Figure 3.5. Effects of  $b$  and  $R_o$  on second natural frequencies

It can be seen from Figure 3.4 that first natural frequencies increase for all height of the beam  $b$ , when catenary parameter  $R_o$  increases. On the other hand, it can be seen from Figure 3.5 that while the second natural frequencies for  $b=20$  mm and  $b=24$  mm changed with respect to catenary parameter  $R_o$  slightly, the second natural frequencies for  $b=28$  mm and  $b=32$  mm decreases.

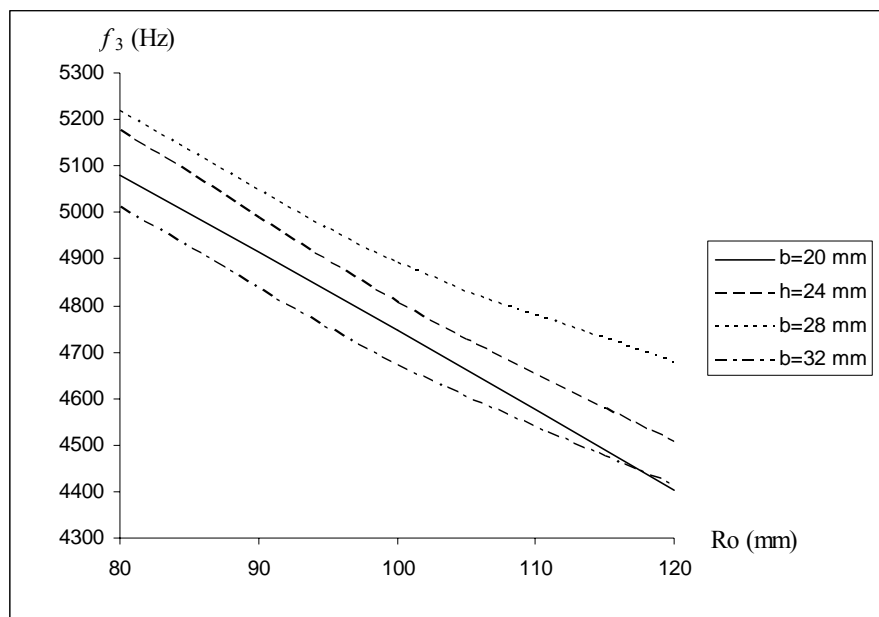


Figure 3.6. Effects of  $b$  and  $R_o$  on third natural frequencies

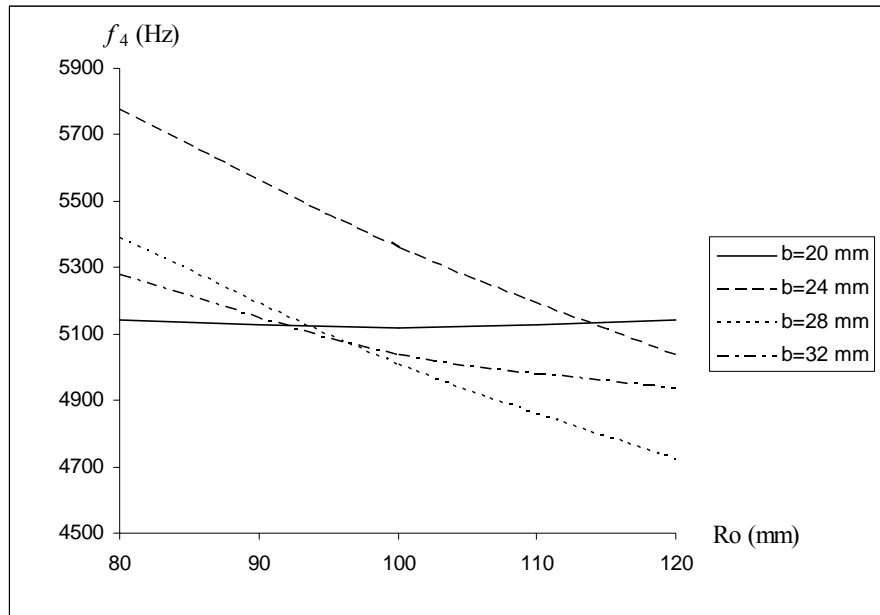


Figure 3.7. Effects of  $b$  and  $R_o$  on fourth natural frequencies

Third natural frequencies shown in Figure 3.6 have the same tendency in the considered range of parameters. Figure 3.7 shows that the frequencies for  $b=20$  mm has different tendency for fourth natural frequencies and the fourth natural frequencies almost equal to each other's for  $b = \{20, 28, 32\}$  mm and  $R_o \approx 93$  mm.

The results shown in Figures 3.4-7 are plotted in Figures 3.8-11 by changing the horizontal axis from  $R_o$  to  $b$ .

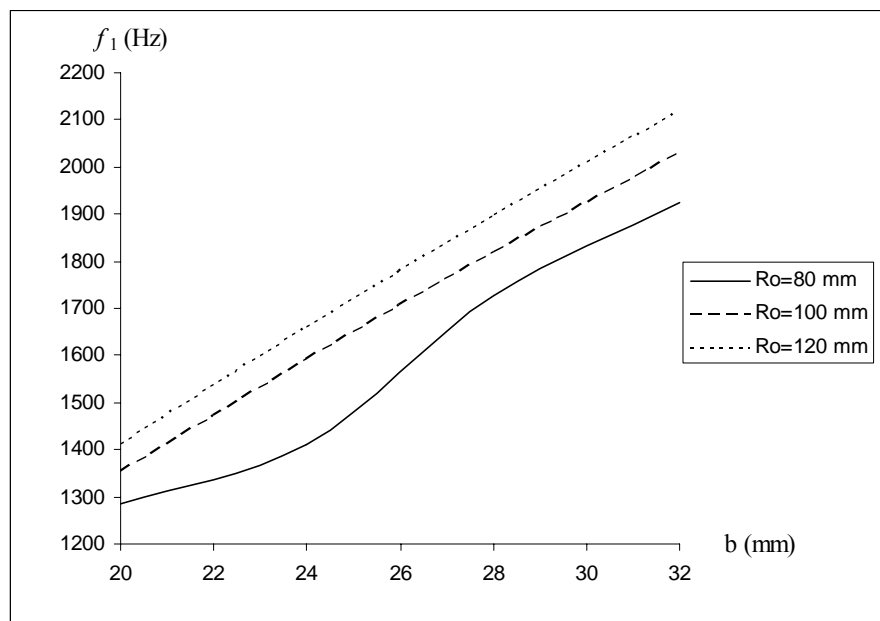


Figure 3.8. Effects of  $R_o$  and  $b$  on first natural frequencies

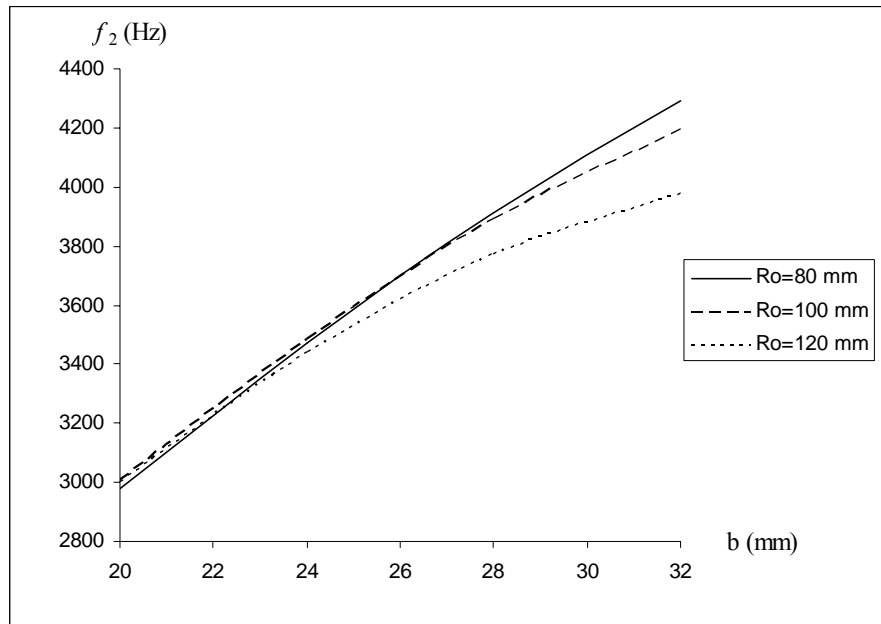


Figure 3.9. Effects of  $R_o$  and  $b$  on second natural frequencies

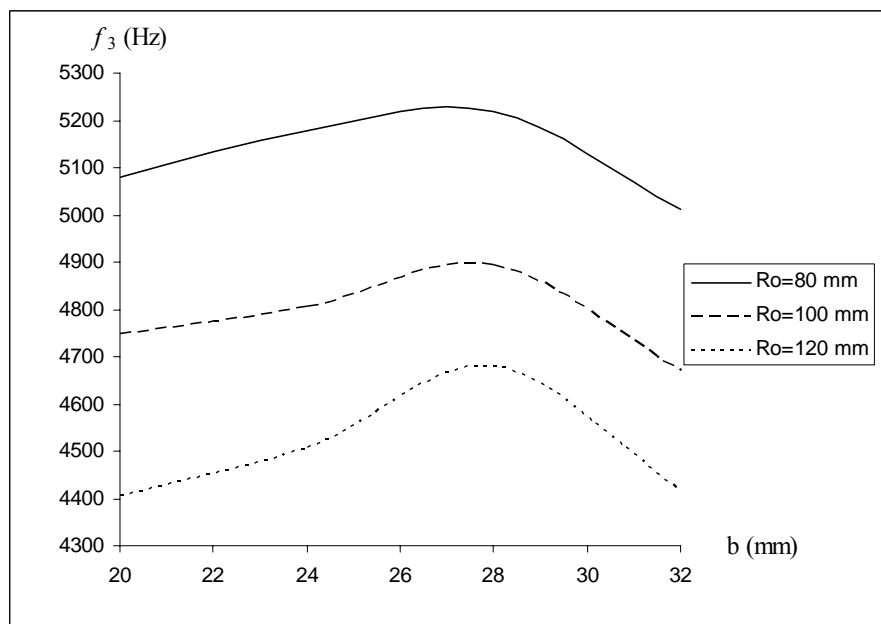


Figure 3.10. Effects of  $R_o$  and  $b$  on third natural frequencies

It can be seen from Figure 3.8 and 3.9 that first and second natural frequencies increase for all catenary parameter  $R_o$ , when height of the beam  $b$  increases, but second natural frequencies are closer to each other until  $b=26$  mm. Third natural frequencies shown in Figure 3. 10 have peak values for  $b=28$  mm and all catenary parameter  $R_o$ .

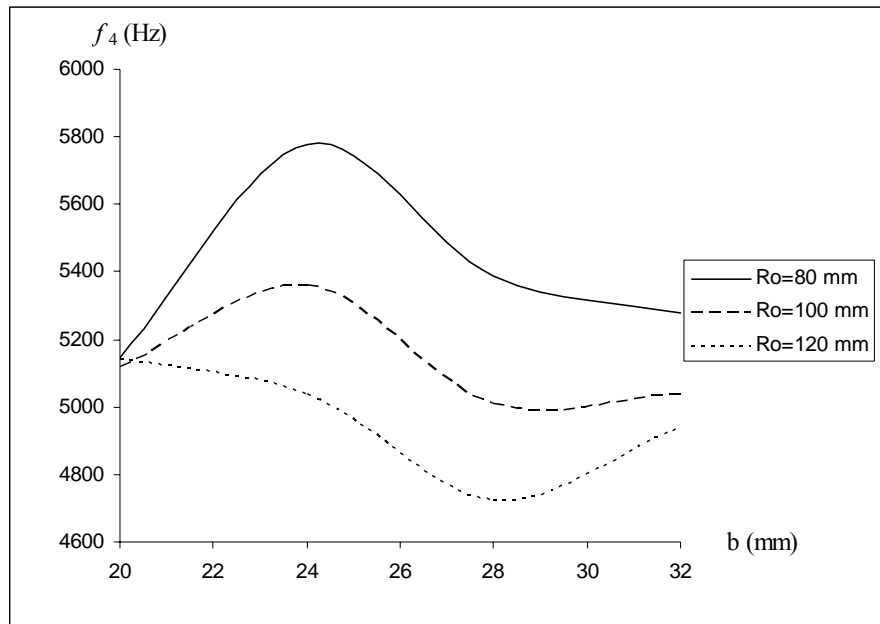


Figure 3.11. Effects of  $R_o$  and  $b$  on fourth natural frequencies

Similar to third natural frequencies, the fourth natural frequencies shown in Figure 3.11 have peak values for  $b \approx 24.5$  mm and  $R_o = \{80, 100\}$  mm. Inverse to this case, the fourth natural frequencies have minimum for  $b \approx 8$  mm and  $R_o = \{100, 120\}$  mm.

From the analysis given above, it is possible to say that in the considered range of parameters, selecting the value of parameters have two alternatives for third and fourth natural frequencies due to the second and third order frequency curves.

Natural vibration mode shapes for a catenary curved beam with the parameters  $b=h=20$  mm,  $R_o=80$  mm, and  $s_1=200$  mm are given in Figures 3.12-3.16.

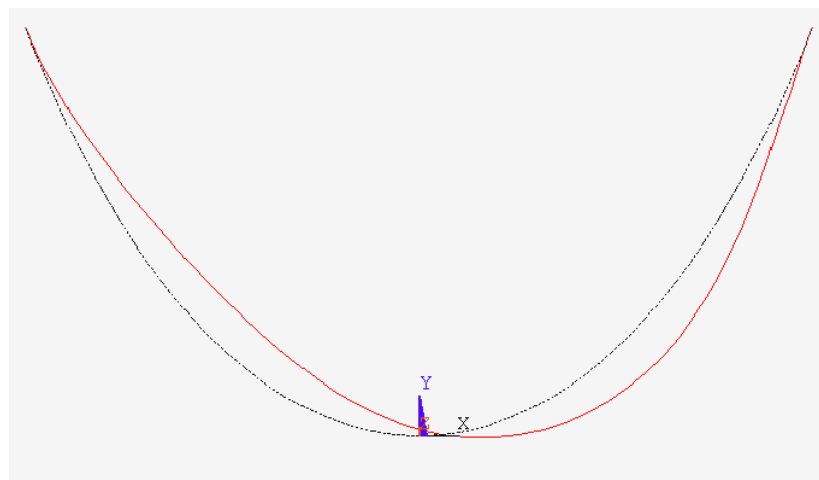


Figure 3.12. First natural mode shape



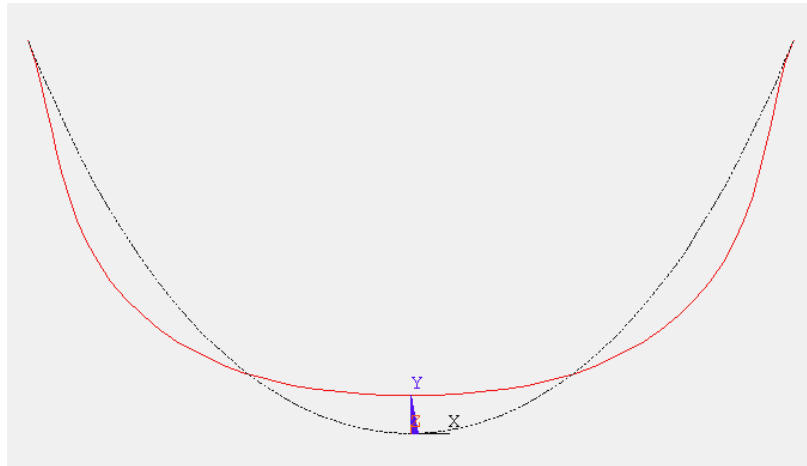


Figure 3.13. Second natural mode shape

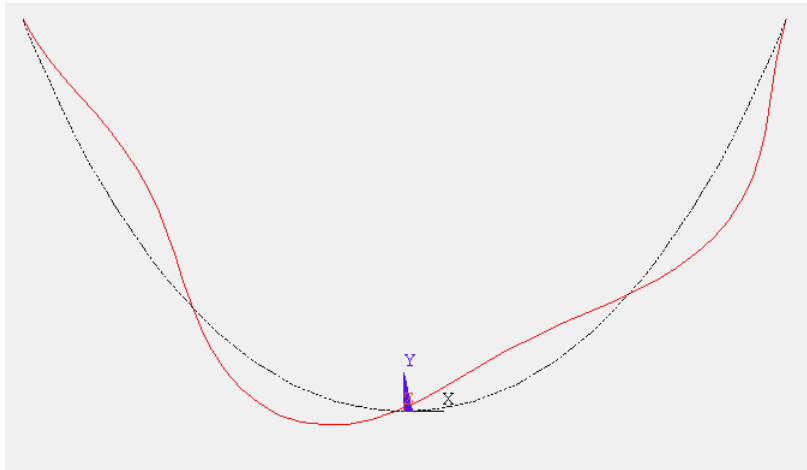


Figure 3.14. Third natural mode shape

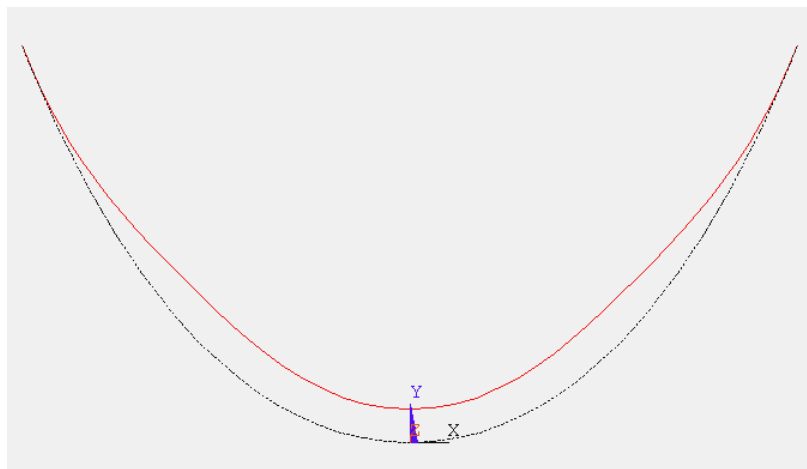


Figure 3.15. Fourth natural mode shape



Figure 3.16. Fifth natural mode shape

## CHAPTER 4

### CONCLUSIONS

In-plane vibration of curved Timoshenko beams with variable curvature is described by a generalized differential eigenvalue problem with variable coefficients. Therefore, numerical methods are used to determine the eigenvalues which are natural frequencies in this problem. To give a variable curvature to curved beam, catenary form is selected due to the most common form in the practice. A computer code is developed in ANSYS which is APDL (ANSYS Parametric Design Language). It is validated by the natural frequencies of Timoshenko circular curved beams with different opening angles available in the literature. After validation of developed computer code, the effects of catenary and cross-section of curved beam parameters on the natural frequencies and mode shapes are studied. Restricting the selected parameter range, it can be concluded that first and natural frequencies show plots almost linear form. However, third and fourth natural frequency plots are in the form of second and third order polynomial functions, respectively.

## REFERENCES

- ANSYS Inc, 2005. ANSYS Commands Reference Release 10.0, Canonsburg PA.
- ANSYS Inc, 2007. ANSYS Elements Reference Release 11.0, Canonsburg PA.
- Chidamparam, P. and Leissa, A.W. 1993. Vibrations of planar curved beams, rings, and arches, *Applied Mechanics Reviews* 46(9): 467-483.
- Den Hartog, J.P., 1928. The lowest natural frequency of circular arcs. *Philosophical Magazine* 5: 400-408.
- Huang, C.S., Tseng, Y.P., Leissa, A.W. and Nieh, K.Y. 1998. An exact solution for in-plane vibrations of an arch having variable curvature and cross section. *International Journal of Mechanical Science* 40: 1159-1173.
- Ibrahimbegovic, A., 1995. On Finite Element Implementation of Geometrically Nonlinear Reissner's Beam Theory: Three-dimensional Curved Beam Elements, *Computer Methods in Applied Mechanics and Engineering* 122: 11-26.
- Irie, T., Yamada, G., and Tanaka, K. 1983. Natural frequencies of in-plane vibration of arches, *Journal of Applied Mechanics* 50: 449-452.
- Kang, K., Bert, C.W., and Striz, A.G. 1995. Vibration analysis of shear deformable circular arches by the Differential Quadrature Method, *Journal of Sound and Vibration* 181: 353-360.
- Kohnke, P., 2004. ANSYS, Inc. Theory Reference. Canonsburg: ANSYS, Inc.
- Love, A.E.H. 1944. A treatise on the mathematical theory of elasticity. New York: Dover Publications.
- Oh, S.J., B.K. Lee, and I.W. Lee. 1999. Natural frequencies of non-circular arches with rotatory inertia and shear deformation. *Journal of Sound and Vibration* 219(1):23-33.
- Petyt, M. 2010. Introduction to finite element vibration analysis. Cambridge: Cambridge University Press.
- Simo, J.C. and Vu-Quoc, L., 1986. A Three Dimensional Finite Strain Rod Model. Part II: Computational Aspects, *Computer Methods in Applied Mechanics and Engineering*. 58: 79-116.
- Timoshenko S.P. 1921. On the correction for shear of the differential equation for transverse vibrations of prismatic bars. *Philosophical Magazine* 41:744-746.

- Tseng, Y.P., Huang, C.S., and Lin, C.J., 1997. Dynamic stiffness analysis for in-plane vibrations of arches with variable curvature, *Journal of Sound and Vibration* 207(1): 15-31.
- Volterra, E. and Morell, J. D. 1960. A note on the lowest natural frequency of elastic arcs, *Journal of Applied Mechanics* 27: 744-746.
- Yardimoglu, B. 2010. Dönen eğri eksenli çubukların titreşim özelliklerinin sonlu elemanlar yöntemi ile belirlenmesi. 2. Ulusal Tasarım İmalat ve Analiz Kongresi, Balıkesir, 514-522
- Yardimoglu, B. 2012. Lecture Notes on Mechanical Vibrations, Izmir: Izmir Institute of Technology.
- Yıldırım, V. 1997. In-plane and out-of-plane free vibration analysis of Archimedes-type spiral springs. *Journal of Applied Mechanics* 64:557-561.